

40.6 Watt, High Power 3.55 GHz Single Crystal XBAW RF Filters for 5G Infrastructure Applications

Ya Shen
Akoustis, Inc.
Huntersville, USA
ashen@akoustis.com

Runqi Zhang
Akoustis, Inc.
Huntersville, USA
rzhang@akoustis.com

Ramakrishna Vetry
Akoustis, Inc.
Huntersville, USA
rvetry@akoustis.com

Jeffrey Shealy
Akoustis, Inc.
Huntersville, USA
jshealy@akoustis.com

Abstract— Previous 4G/LTE applications for RF BAW filters were predominately focused on relatively low power, sub-3 GHz filters for wireless applications. Emerging 5G infrastructure applications bring new requirements for high-power, high-frequency micro RF filters to address coexistence challenges in newly license bands (n77, n78, n79) in the 3.3 to 5 GHz spectrum. This work focuses on the power robustness of 3.5-3.6 GHz XBAW band-pass RF filters constructed using single crystal and poly crystal piezoelectric (“piezo”) layers. Superior power handling as well as small-signal performance has been demonstrated.

Keywords— BAW filters, acoustic filters, single crystal AlN thin film, poly crystal AlN thin film, mobile communication, LTE, 5G, power handling.

I. INTRODUCTION

For the past a few decades, surface acoustic wave (SAW) based filters and bulk acoustic wave (BAW) based filters have been dominating the RF filter market, due to their undeniable superiorities: low insertion loss, high rejection, small form factor, and compatibility with large-scale semiconductor manufacturing process for low cost. With the accelerated expansion of wireless communication worldwide, frequency bands in the 3-6 GHz have become a primary focus of research and development in the RF filter industry. As an extension to the current Long-Term Evolution (LTE) bands operating at sub 2.7 GHz, the newer 3.4 – 3.8 GHz range has attracted a lot of interest, namely TDD Band 42 and Band 43. Additionally, the emerging 5G bands also have n77 and n78 in similar frequency range. A number of institutions have demonstrated the capability of designing and manufacturing SAW and BAW filters in the 3 GHz frequency range [1]-[5].

Single-crystalline AlN thin film grown by metal organic chemical vapor deposition (MOCVD) has better crystalline alignment compared to poly-crystalline AlN thin film grown by physical vapor deposition (PVD), as its full-width half-maximum (FWHM) measured by (0002) X-ray diffraction (XRD) is 0.057° , contrasted to about 1.6° of FWHM typically for poly-crystalline AlN thin films. This significantly lower FWHM defines crystal quality and can lead to 3x higher thermal conductivity in Si thin films [6]. Furthermore, the authors observed marginally higher longitudinal acoustic velocity in the single-crystalline AlN thin films compared to poly-crystalline AlN thin films, which allows slightly thicker AlN thin film to be used for the resonators working at the same frequency. In addition, it has been reported that thicker AlN

thin film improves thermal conductivity [7]. This better alignment of crystalline structure is also believed to be the source for lower loss, lower power consumption and higher thermal conductivity, which in turn allows single-crystal-AlN-based BAW filters to improve insertion loss and boost power handling capability [8].

II. DEVICE AND RF FILTER FABRICATION AND PACKAGING

The focus of this study is on single-crystal-AlN-based BAW resonators and filters. Single crystal AlN thin film was grown by MOCVD. An 11-level mask was used to produce the XBAW resonators with dual air interfaces (Fig 1). A unique MEMS process [8] enabled the manufacturing of the final devices on a 150-mm diameter silicon substrate. For comparison, BAW resonators and filters were fabricated with poly-crystal-AlN thin film, which is sputtered by PVD. These devices used the same mask plates, substrates, and followed the same fabrication process as that of the single crystal devices.

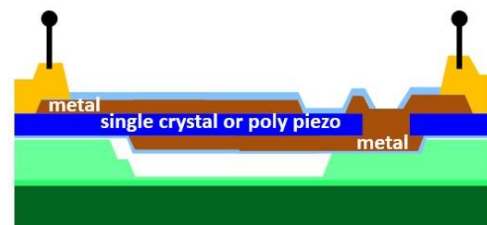


Fig. 1. Cross-section of a XBAW resonator device.

The resulting filter die with an area less than 1mm^2 was packaged in a $5\times 5\text{mm}^2$ laminate and mounted on an evaluation board (Fig 2), then measured with a vector network analyzer (VNA). As a self-matched prototype product, surface mounted devices (SMDs) have been mounted on the laminate for matching and tuning purposes.

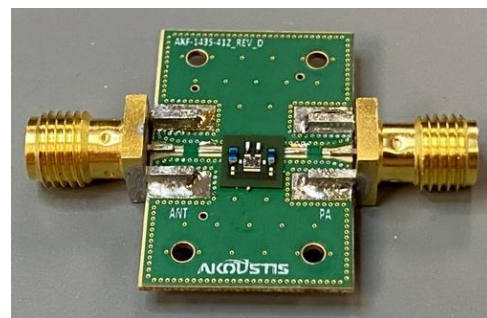
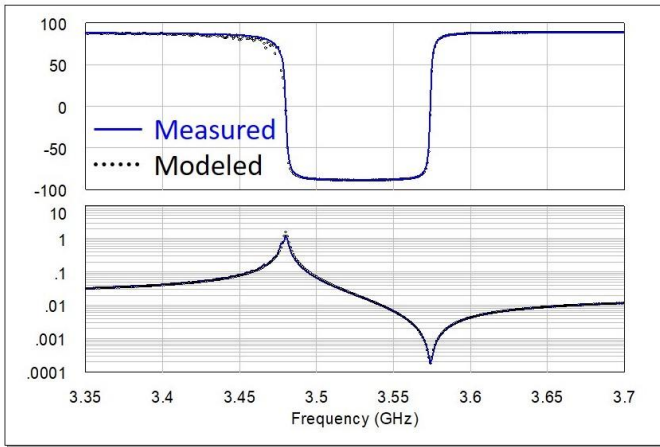


Fig. 2. 3.55 GHz RF BAW filter mounted on laminate and evaluation board.

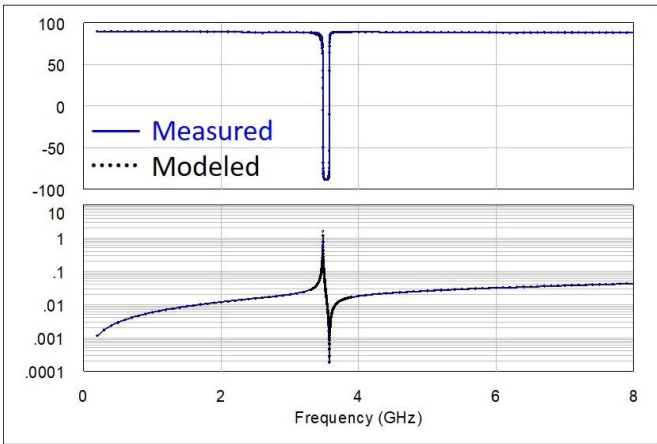
III. RESULTS AND DISCUSSION

A. Resonator Modeling and Small Signal Measurement

A modified Butterworth Van-Dike (mBVD) model has been extracted with on-wafer resonator 1-port probe measurement. Open-short de-embedding has been applied to obtain the intrinsic resonator performance. A comparison of modeled and measured resonator Y11 magnitude and phase is plotted in Fig 3. Measured resonant frequency (f_s) and anti-resonant frequency (f_p) at the zero-phase crossing is 3.48 GHz and 3.574 GHz respectively. Bode Q of the same resonator is plotted in Fig 4 [9]. Extracted Q_{max} , Q_s , Q_p and k_{eff}^2 are 2778, 1541, 2036 and 6.32% respectively. This translates to a figure of merit of 175 at 3.534 GHz.



(a) Narrow-band



(b) Wide-band

Fig. 3. Narrow-band and Wide-band comparison of resonator measurement and mBVD model in both phase and magnitude.

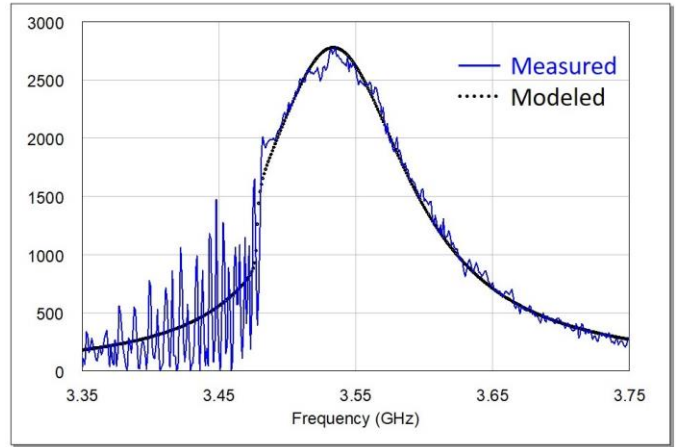


Fig. 4. Bode plot comparing measured and modeled resonator showing Q-factor versus frequency [9].

B. Filter Simulation and Small Signal Measurement

A BAW ladder-type filter has been designed with the mBVD model extracted from resonators. An HFSS 3-D model of the filter die with laminate package and SMD ports is shown in Fig 5. Modeled and measured filter S21 is overlaid in Fig 6. Insertion loss of 1.2 dB minimum and 1.4 dB average have been reported, with an absolute 3-dB bandwidth of 120 MHz.

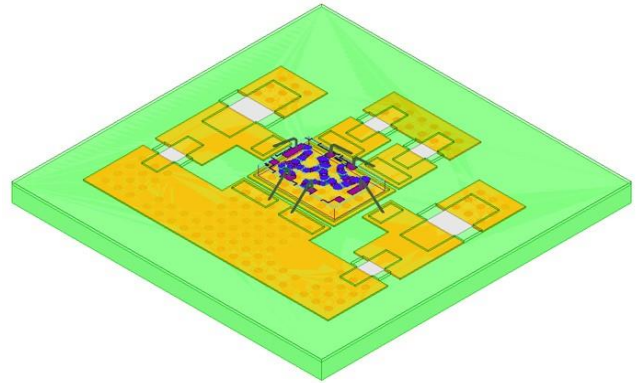


Fig. 5. HFSS 3D model of 3.55 GHz RF BAW filter: filter die on laminate with SMD ports.

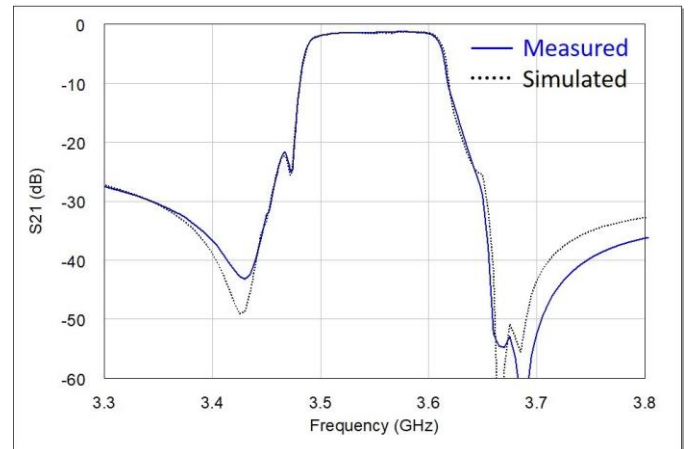


Fig. 6. Simulated and measured 3.55 GHz bandpass filter, with in-band return loss better than -16 dB across passband.

For comparison purpose, the S21 of a single-crystal-AIN-based BAW filter and that of a poly-crystal-AIN-based BAW filter are both plotted in Fig 7. As both filters used the same mask plates, went through the same fabrication process, and packaged in the same laminate, wide-band performance is very comparable. The main observable difference in small signal is an approximately 0.2 dB passband average insertion loss improvement of the single-crystal-AIN-based BAW filter.

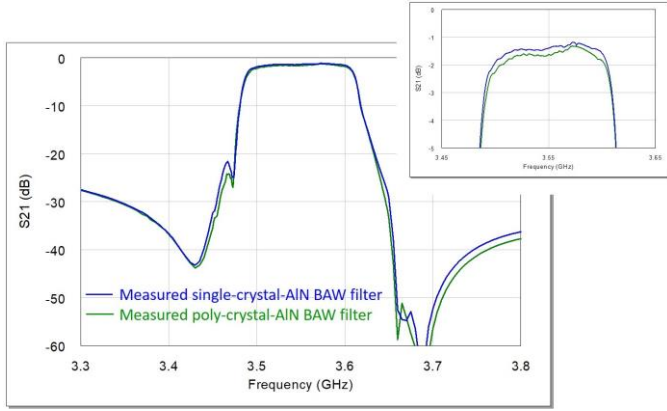


Fig. 7. Measured 3.55 GHz single-crystal-AIN and poly-crystal-AIN bandpass BAW filters.

C. Filter Power Testing and Comparison

Power tests with identical condition were conducted on both single-crystal-AIN-based BAW filters and poly-crystal-AIN-based BAW filters. A pulsed signal with 1% duty cycle and 800um period was applied at both the middle and the upper edge of the passband. Near the band center, the peak power handling capability of single crystal filters was 44.8 W / 46.6 dBm. Near the right edge of the passband (Fig. 8), the best single crystal peak power capability was 40.6W / 46.1 dBm, which was 18.1 W higher than the best poly crystal filter capability of 22.5W / 43.5 dBm.

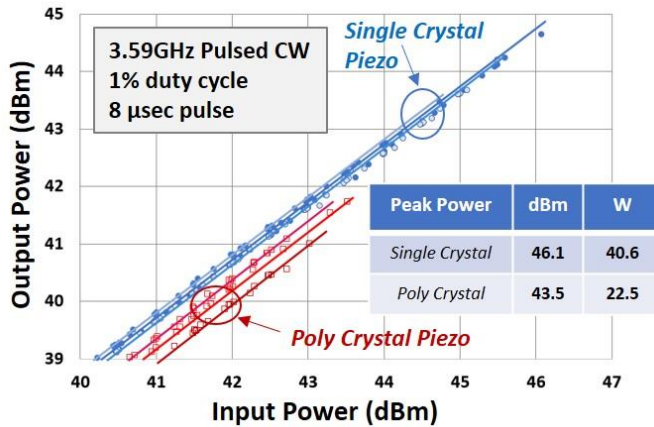


Fig. 8. Measured power sweep at right band edge of 3.55 GHz XBAW filter for single crystal and poly crystal piezo types.

The insertion loss under RF drive (Fig. 9) for the single crystal piezo filters ranged from 1.2 to 1.4 dB compared to 1.6 to 2.0dB for the poly crystal piezo filters.

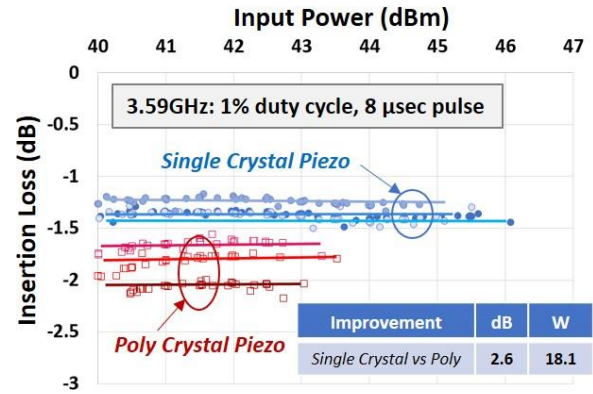


Fig. 9. Measured insertion loss of 3.55 GHz filters versus input power for single crystal and poly crystal piezo types. Filters failed after last data point.

IV. CONCLUSION

BAW filters operating at center frequency of 3.55 GHz with an absolute 3-dB bandwidth of 120 MHz were designed, fabricated and measured, where the single-crystal-AIN-based BAW filter is compared with the poly-crystal-AIN-based BAW filter. The single-crystal-AIN-based BAW filter exhibited 2.6 dB or 18.1 W higher power handling capability, as well as an approximately 0.2 dB improvement in insertion loss. This improvement in power handling and small signal measurement is attributed to the different AIN material used during fabrication of these filters. To the authors' knowledge, this is the highest reported BAW RF filter power handling capability at the mid-3GHz frequency range. This expands the application space of BAW filters for higher power demands.

REFERENCES

- [1] Tetsuya Kimura ; Masashi Omura ; Yutaka Kishimoto ; Kenya Hashimoto, "Comparative Study of Acoustic Wave Devices Using Thin Piezoelectric Plates in the 3-5-GHz Range," IEEE Transactions on Microwave Theory and Techniques, 2019, Volume 67, Issue 3
- [2] Yuichi Takamine, Tsutomu Takai, Hideki Iwamoto, Takeshi Nakao and Masayoshi Koshino, "A Novel 3.5 GHz Low-Loss Bandpass Filter Using I.H.P. SAW Resonators", 2018 Asia-Pacific Microwave Conference (APMC).
- [3] Qingrui Yang, Wei Pang, Daihua Zhang, Hao Zhang, "A Wide band Bulk Acoustic Wave Filter with Modified Lattice Configuration", 2015 IEEE MTT-S International Microwave Symposium.
- [4] Tuomas Pensala, Tapani Makkonen, James Dekker and Markku Ylilammi, "Laterally Acoustically Coupled BAW filters at 3.6 GHz", 2018 IEEE International Ultrasonics Symposium (IUS)
- [5] Jeffrey B. Shealy, Ramakrishna Veturu, Shawn R. Gibb, Michael D. Hodge, Pinal Patel, Michael A. McLain, Alexander Yu. Feldman, Mark D. Boomgarden, Michael P. Lewis, Brook Hosse and Rohan Holden, "Low Loss, 3.7GHz Wideband BAW Filters, Using High Power Single Crystal AIN-on-SiC Resonators", 2017 IEEE MTT-S International Microwave Symposium (IMS).
- [6] Ju et. al., JAP, Sep 2011.
- [7] S.R.Choi, "Thermal Conductivity of AIN and SiC Thin Films" Int. Jo. of Thermophysics, p896, 2006
- [8] R. Veturu, M.D. Hodge and J.B. Shealy, "High Power, Wideband Single Crystal XBAW Technology for sub-6 GHz Micro RF Filter Applications", 2018 IEEE International Ultrasonics Symposium (IUS).
- [9] R. Ruby, R. Parker, D. Feld, "Method of Extracting Unloaded Q Applied Across Different Resonator Technologies", Proc. of IEEE Ultrason. Symp., pp1815-1818, 2008.

